

1N-88  
198587  
30P

# Demonstration of the Feasibility of an Integrated X-Ray Laboratory for Planetary Exploration

E. D. Franco, J. A. Kerner, L. N. Koppel, and M. J. Boyle

(NASA-CR-177631) DEMONSTRATION OF  
THE FEASIBILITY OF AN INTEGRATED X  
RAY LABORATORY FOR PLANETARY  
EXPLORATION (Advanced Research and  
Applications Corp.) 30 p

N94-24832

Unclass

G3/88 0198587

CONTRACT NAS2-13416  
December 1993

**NASA**

National Aeronautics and  
Space Administration



# **Demonstration of the Feasibility of an Integrated X-Ray Laboratory for Planetary Exploration**

E. D. Franco, J. A. Kerner, L. N. Koppel, and M. J. Boyle

Advanced Research and Applications Corporation  
425 Lakeside Drive  
Sunnyvale, CA 94086

Prepared for  
Ames Research Center  
CONTRACT NAS2-13416  
December 1993



National Aeronautics and  
Space Administration

**Ames Research Center**  
Moffett Field, California 94035-1000

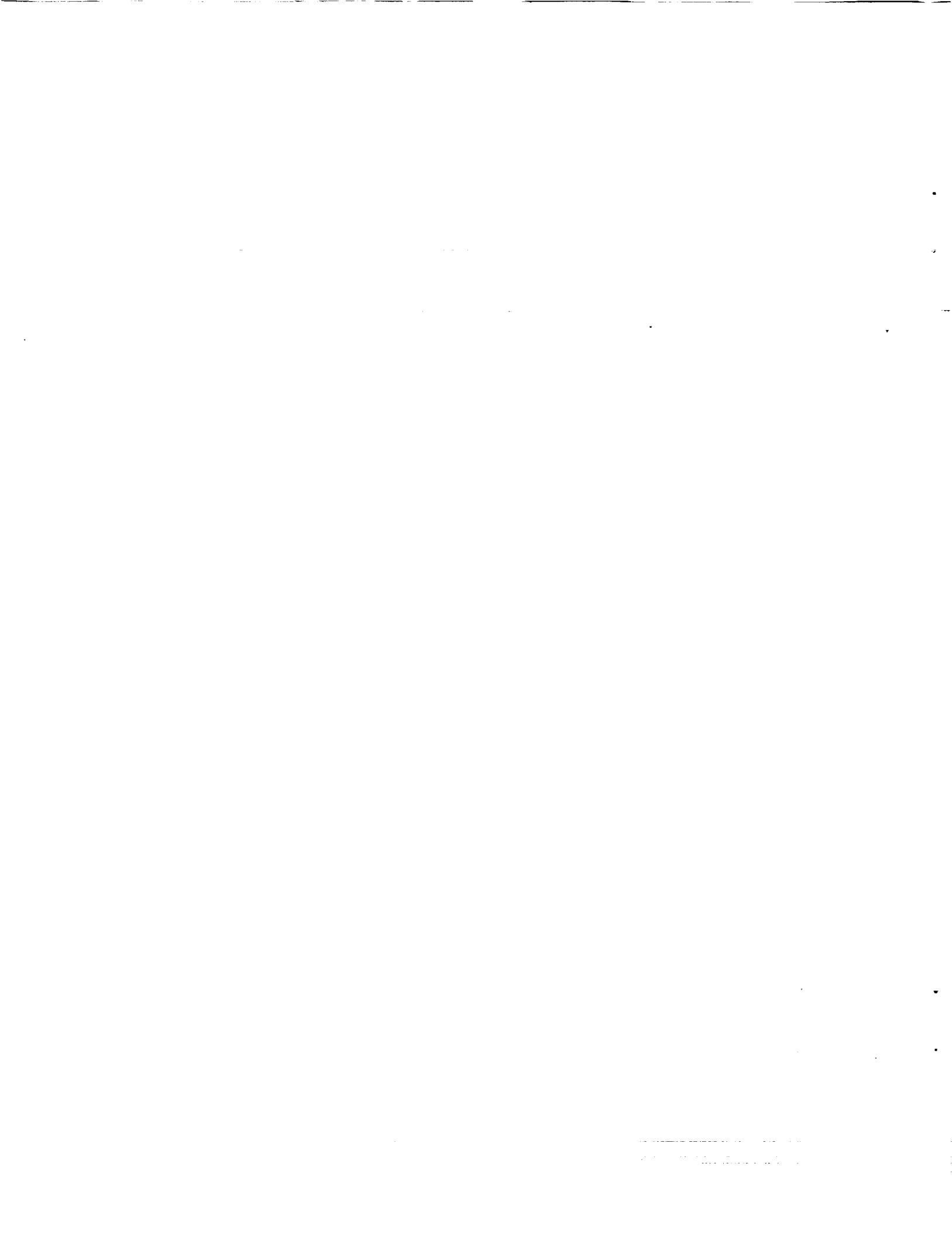


# TABLE OF CONTENTS

Sections	Page
EXECUTIVE SUMMARY .....	1
ACKNOWLEDGMENTS.....	1
1.0 INTRODUCTION .....	2
1.1 Science Background .....	2
1.2 Science and Technical Breadboard Requirements .....	3
1.3 Planetary Exploration Constraints .....	4
2.0 TECHNICAL APPROACH .....	5
2.1 X-Ray Diffraction/fluorescence Breadboard Module .....	5
2.2 Light Element X-Ray Fluorescence Breadboard Module .....	8
2.3 Supporting Subsystems.....	10
3.0 BREADBOARD DEMONSTRATION .....	11
3.1 X-ray Diffraction Breadboard Results .....	11
3.2 X-Ray Fluorescence Breadboard Results.....	19
3.3 Compatibility with Planetary Exploration Constraints .....	22
4.0 CONCLUSIONS/RECOMMENDATIONS .....	24
5.0 REFERENCES.....	26

## LIST OF FIGURES

Figures	Page
1. The x-ray diffraction/fluorescence breadboard module. ....	6
2. Calculated d-spacing resolution for the diffraction breadboard module.....	7
3. Multilayer bandpass response for carbon.....	9
4. The light element x-ray fluorescence breadboard module.....	10
5. Breadboard x-ray diffraction examination of halite.....	12
6. Breadboard x-ray diffraction examination of montmorillonite. ....	13
7. Breadboard x-ray diffraction examination of 50% palagonite.....	15
8. Breadboard x-ray diffraction examination of 80% palagonite.....	15
9. Breadboard x-ray diffraction examination of 90% palagonite.....	16
10. Breadboard x-ray fluorescence examination of montmorillonite.....	20
11. Demonstration of bandpass rejection of oxygen. ....	20
12. Carbon signal as a function of concentration.....	21

## LIST OF TABLES

	Page
1. Planetary mission instrument constraints. ....	4
2. Observed and tabulated montmorillonite d-spacings. ....	13
3. Crystalline test matrix. ....	14
4. Observed and tabulated d-spacings in 50% palagonite sample.....	17

## EXECUTIVE SUMMARY

The identification of minerals and elemental composition is an important component in the geological and exobiological exploration of the solar system. X-ray diffraction and fluorescence are common techniques for obtaining these data. This project demonstrated the feasibility of combining these analytical techniques in an integrated x-ray laboratory compatible with the volume, mass, and power constraints imposed by many planetary missions. In this project, breadboard level hardware was developed to cover the range of diffraction lines produced by minerals, clays, and amorphous; and detect the x-ray fluorescence emissions of elements from carbon through uranium. These breadboard modules were fabricated and used to demonstrate the ability to detect elements and minerals. Additional effort is required to establish the detection limits of the breadboard modules and to integrate diffraction and fluorescent techniques into a single unit. We conclude that this integrated x-ray laboratory capability will be a valuable tool in the geological and exobiological exploration of the solar system.

## ACKNOWLEDGMENTS

The development of a new technology is always challenging and exciting. This is especially so when the application for this technology is on other planets and moons of the solar system rather than our home planet Earth where our previous experience resides. In large part, the success of this project is the result of the guidance, support, and collaboration provided by a number of individuals affiliated with the NASA Ames Research Center. In particular, we gratefully acknowledge the guidance and support provided by Mr. Glenn Carle and Mr. Mark Fonda of NASA Ames Research Center, by Dr. John Marshall, Ms. Deborah Schwartz-Kolyer, and Dr. Rocco Mancinelli of the SETI Institute; and the insight into the Martian geology provided by Dr. Amos Banin of the University of Tel Aviv.

## 1.0 INTRODUCTION

This final report was prepared in the partial fulfillment of NASA Contract Number NAS2-13416, a Small Business Innovative Research (SBIR) Phase II project. This project "An Integrated-Function X-Ray Laboratory for the Geological and Exobiological Exploration of Mars" was administered by the NASA Ames Research Center. The period of performance was from September 1991 through January 1993.

### 1.1 Science Background

The surface rocks and materials of a planet contain a record of its evolution. The chemistry, mineralogy, texture, and geological relationships of these materials provide information on major events such as planetary accretion and global differentiation, and magmatic, sedimentary, metamorphic, and aeolian processes. Information can be obtained on the timing of events, the environment of deposition, and the overall geologic processes occurring on the planet.

The planet Mars is of great scientific interest since it is very similar to Earth.<sup>1</sup> Geologic and climatological studies have suggested that the early Martian environment may have been very similar to that of early Earth. Both planets show histories of liquid surface water, warmer temperatures, cometary and meteoric impacts, as well as relatively thick carbon dioxide and nitrogen atmospheres and volcanic activity. Studying Mars helps us to understand events that occurred while life was originating on Earth.

The Mars Science Working Group, established by the NASA Headquarters Solar System Exploration Division, has stated that a primary science goal associated with the continued exploration of Mars is to better establish the chemical and physical characteristics of the Martian surface.<sup>1</sup> The Committee on Planetary and Lunar Exploration (COMPLEX) of the National Academy of Sciences recommended an "intensive study of local areas to establish the chemical, mineralogical, and petrological character of different components of the surface material and to determine the distribution, abundance, sources and sinks of the volatile materials including an assessment of the biologic potential now and during the past epochs."<sup>2</sup>

The importance of Mars has led NASA to pursue a combination of remote sensing investigations (in the near term) with the Mars Observer Mission and *in situ* measurements (around the turn of the century) with the proposed MESUR Mission.<sup>3</sup> The Mars Observer Mission will determine, on a

global basis, the chemical and mineralogical distribution and provide the basis for selecting candidate sites for *in situ* measurements. At these sites, geologists and exobiologists will be interested in mineral and elemental analysis of the surrounding rocks and soils. This analysis will provide evidence of the paleohydrological events, pre-biotic chemical evolution, volcanism, plutonism, impact processes, and the sedimentological and weathering processes that are important for understanding the evolution of Mars.

## 1.2 Analytical X-Ray Technical Requirements

The geological and exobiological issues discussed above suggest the need for a tool that provides mineral and elemental identification data and the subsequent quantification of their concentrations. This project considered whether x-ray diffraction and fluorescence, two major analytical techniques in geology, could be combined to produce an integrated x-ray laboratory compatible with planetary exploration.

X-ray diffraction produces unique fingerprints of minerals and crystals under examination and can be used to determine the fraction of amorphous material in the sample. Similarly, x-ray fluorescence produces unique fingerprints of elements under examination. This technique is divided between standard range x-ray fluorescence that covers the elements heavier than oxygen, and light element x-ray fluorescence that considers elements from beryllium to oxygen. The light elements include the biogenic elements such as carbon, nitrogen, and oxygen.

The x-ray diffraction measurement must be able to cover essentially all of the known minerals in order to produce data that is relevant to geological and exobiological planetary exploration missions. On Earth, almost 98 percent of all of the minerals and crystals have characteristic d-spacings in the range from 1.5 to 20 Å<sup>4</sup>. In particular, the d-spacing range from 1.5 to 5 Å contains the primary diffraction lines of the salts and silicates. The region from 5 to 20 Å contains the primary diffraction lines of clays. Amorphous materials, when examined by diffractometry, do not produce sharp diffraction lines but rather produce broad regions of low intensity in the 1.5 to 20 Å d-spacing range. In the context of Martian *in situ* analysis, the instrument performance requirements for the diffraction measurements may be summarized as:

- 1) Cover a range of d-spacings from 1.5 to 20 Å
- 2) Detect minerals in a concentration greater than 1 percent by weight
- 3) Detect amorphous materials in a concentration greater than 10 percent by weight
- 4) Require minimal sample preparation.

Similarly, x-ray fluorescence produces unique fingerprints of elements under examination. This technique is divided between standard range x-ray fluorescence that covers the elements heavier than oxygen, and light element x-ray fluorescence that considers elements from beryllium to oxygen. The light elements include the biogenic elements such as carbon, nitrogen, and oxygen. In the context of Martian *in situ* analysis, the instrument performance requirements for the fluorescence measurements may be summarized as:

- 1) Cover the range of elements from carbon through uranium
- 2) Detect elements in a concentration greater than 100 ppm in a complex mineral matrix
- 3) Require minimal sample preparation.

### 1.3 Planetary Exploration Constraints

X-ray fluorescence and diffraction are well established analytical techniques that have only partially been applied to the planetary exploration of the solar system. For example, standard x-ray fluorescence has been applied with notable success in the *in situ* study of the Moon and Mars(REFERENCE). X-ray diffraction has not been extended to planetary exploration and there has never been an integrated x-ray laboratory capability developed for *in situ* planetary exploration.

X-ray diffraction typically requires highly precise instruments that are large, bulky, and complicated and that consume about a kW of electrical power. At a minimum, however, instruments designed for planetary exploration must conform to stringent mass, power and volume budgets. For this project, design targets previously proposed for the Mars Environmental Survey (MESUR) mission were used to guide our development of the integrated x-ray laboratory and are listed in table 1.<sup>5</sup> Future work will address the many other mission specific constraints such an instrument must comply with before being declared flight ready.

TABLE 1. ENGINEERING DESIGN REQUIREMENTS.

Parameter	Value
Mass	≤ 2.5 kg
Volume	≤ 0.1 m <sup>3</sup>
Power	≤ 15 W
Operating Time	≤ 4.5 hours

## 2.0 TECHNICAL APPROACH

Breadboard level hardware was designed and fabricated to demonstrate the plausibility of integrating the x-ray diffraction and fluorescence techniques into an instrument compatible with planetary exploration. This allowed us to empirically determine the impact of a compact geometry, low power, and minimal sample preparation on the quality of the fluorescence and diffraction data. Two breadboard modules were produced to separately examine these parameters for x-ray diffraction/fluorescence and light element fluorescence. This division was made on the basis of differences in detector and source technology necessary for these measurements. There is no fundamental reason why these modules cannot be integrated into a single instrument package. The breadboard modules are described in the following sections.

### 2.1 X-Ray Diffraction/Fluorescence Breadboard Module

The primary challenge for this module is associated with implementing x-ray diffraction in a compact, low power configuration. Commercial diffractometers typically have a radius on the order of 20 cm, to achieve good d-spacing resolution, and are often equipped with carefully aligned monochromators to reduce the background. These units typically utilize electrical x-ray tubes that have characteristic power levels of a kW.

The x-ray diffraction/fluorescence breadboard module is shown in figure 1. Our approach combined the standard x-ray fluorescence and diffraction analytical techniques into a single module as a step towards integration. A major innovation of our approach was to use a thinned, backside illuminated charge coupled device (CCD) as an imaging detector as well as a spectrally resolving detector. This allowed us to combine the fluorescence and diffraction functions and reduce the mass and power of accomplishing these functions.

The module is composed of an iron target x-ray tube, a cadmium-109 isotopic source and the CCD detector. During operation of the x-ray tube, the diffraction pattern and the x-ray fluorescence spectrum of the elements from silicon to chromium are collected simultaneously. The 10 mCi cadmium-109 source produces 22.2 keV x-ray emission that will excite the K-shell emission of all elements below ruthenium ( $Z=44$ ) and the L-shell emissions through uranium ( $Z=92$ ).

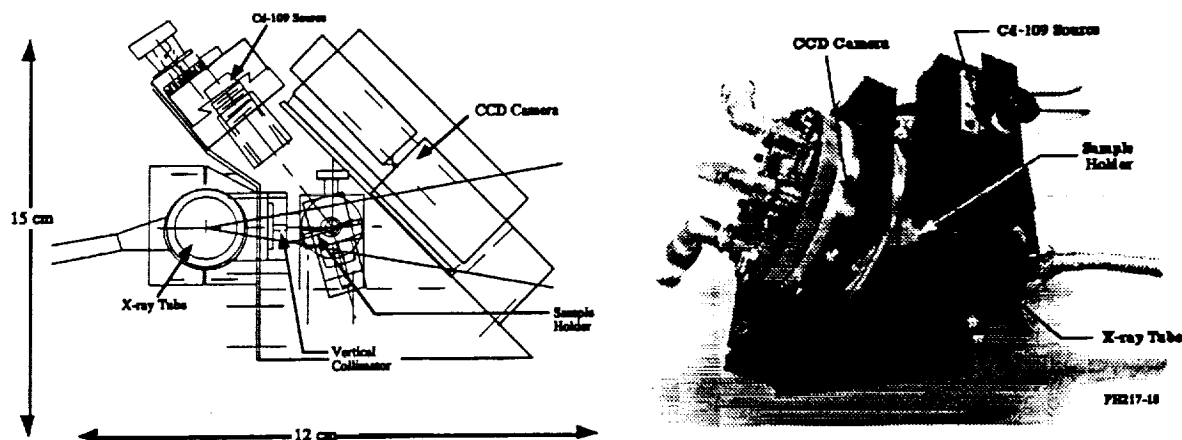


Figure 1.- The x-ray diffraction/fluorescence breadboard module.

The CCD and the x-ray tube are configured in a non-scanning "powder camera" geometry with a radius of 3.8 cm. A CCD with a 512 x 512 array of 27  $\mu\text{m}$  pixels was selected for this demonstration. A CCD of this size, however, could not cover the entire angular range corresponding to a d-spacing from 1.5 to 20  $\text{\AA}$ . In the breadboard, we covered this range in several steps by manually moving the CCD. Increasing the size of the CCD to an array of 1024 x 1024 pixels will cover the required d-spacing range.

An iron x-ray tube, with a maximum power rating of only 9 W, was selected for this application to keep the diffraction measurement under 4.5 hours, the duration of a Martian night. The output of the x-ray tube was filtered with a manganese K-edge filter to create an essentially monochromatic iron x-ray beam for diffraction and fluorescence. Both the iron x-ray tube and the cadmium-109 isotopic source are compatible with use for an actual Martian mission.

A key design driver for the diffraction camera was the d-spacing resolution required to observe the diffraction lines characteristic of the minerals present in a complex sample. The resolution of the powder camera is defined by the apparent size of the x-ray source established by the source-to-sample distance, vertical collimation, the distance from the sample to the detector, and the sample tilt angle. The calculated d-spacing resolution of the powder camera is shown in figure 2. The region of highest resolution corresponds to the expected location of the important diffraction lines for salts and silicates. Here, the d-spacing resolution is greater than 30 over the d-spacing range from 1.5 to 5  $\text{\AA}$ . Diffraction lines that are separated by more than 3 percent should be observed in

this range. The d-spacing region corresponding to clays is characterized by a d-spacing resolution below 10.

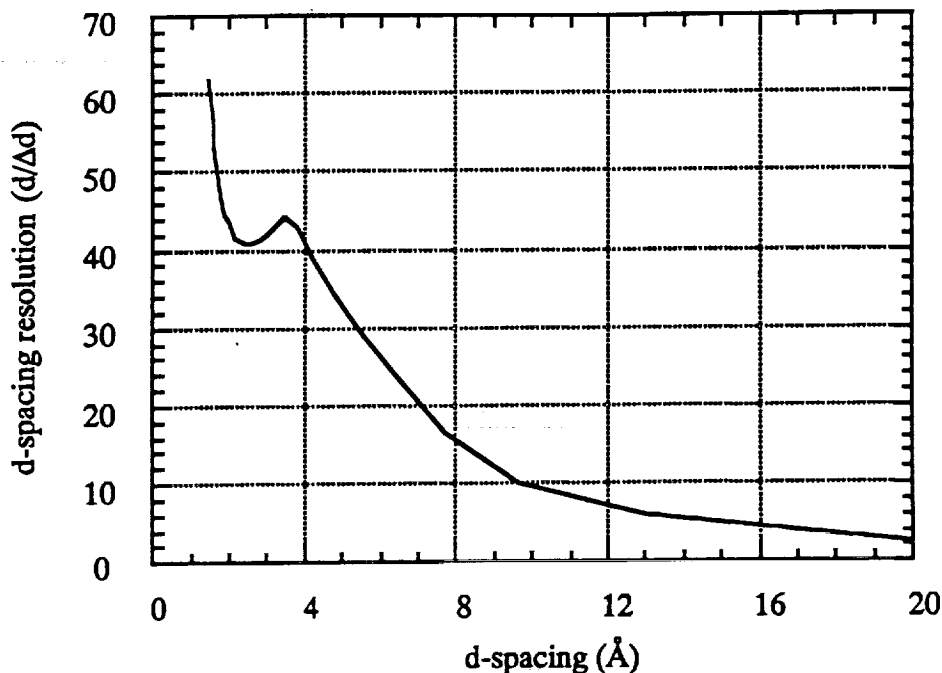


Figure 2.- Calculated d-spacing resolution for the diffraction breadboard module.

The incident x-ray beam must sample a large number of randomly oriented mineral grains in order to produce a diffraction signal proportional to mineral concentration. This requirement is traditionally met by either spatially averaging the signal over a large number of grains, or by temporally averaging the signal while the sample is rocked or rotated. The compact powder camera geometry requires the temporal averaging method, which was not implemented at this stage of feasibility demonstration due to budget constraints. Thus, this breadboard module could be used only to identify the presence of minerals, but not their concentration, within a sample.

The data recorded by the CCD is made up of diffraction and fluorescent information. The location of the diffraction pattern upon the two-dimensional image plane of the CCD can be directly related to a candidate diffraction event. The magnitude of the signal in a given CCD pixel is related to the energy of the photon that created that response. We developed techniques which distinguish whether events recorded by the CCD were produced by diffracted or fluorescent radiation. The events that had an energy corresponding to the characteristic iron x-ray produced by the x-ray tube were classified as a diffraction event. The other events are sorted by energy and then used to form a fluorescence spectrum.

No special sample preparation techniques were implemented for the breadboard other than those required to approximate the Martian soil (typically made up of extremely fine sand). Our samples were simply mechanically ground and then sieved to remove all particles whose diameter was greater than about 100  $\mu\text{m}$ . The sample was then loaded into the sample holder and flattened with a straight edge. The sample mass required to perform the diffraction and fluorescence measurement was of the order of 10 mg.

## **2.2 Light Element X-Ray Fluorescence Breadboard Module**

The challenge for the detection of light elements by fluorescence is to overcome their relatively inefficient x-ray production. This leads to poor signal-to-noise ratios, relatively long assay times, and values for the lower detection limits that can be much greater than 100 ppm.

On Mars, carbon and nitrogen measurements are further complicated by large concentrations of oxygen. Viking indicated that approximately 45 percent of the Martian regolith is composed of oxygen and that less than 1 percent is nitrogen or carbon.<sup>6</sup> Thus, the primary issue addressed here was how to extract the carbon and nitrogen radiation from a large oxygen background.

Our approach relied on alpha particles to excite the characteristic radiation of the light elements and figured x-ray multilayer optics to provide spectral discrimination and background rejection. Alpha particle excitation was selected since it is more efficient than electron or x-ray excitation, in generating fluorescent radiation from light elements.

Multilayer optics are fabricated by depositing thin alternating layers of two elements that differ significantly in their indices of refraction in the x-ray spectral region onto a smooth substrate. Layer thicknesses are comparable to the x-ray wavelengths and there is a well-defined relationship between the radiation angle of incidence and the reflection properties of the multilayer coating.

The multilayer coating can be designed to act as a bandpass filter that selectively transports carbon or nitrogen radiation and suppress the oxygen background. Multilayer coatings can be applied to a number of substrates, including figured substrates, to produce a variety of focusing and collection optical geometries. This improves the signal-to-noise ratio and leads to detection of carbon and nitrogen with enhanced sensitivity. Additionally, this approach allows us to consider non-energy resolving detectors for the detection of light element x-ray fluorescence, ultimately simplifying the data acquisition chain for the integrated x-ray instrument.

The breadboard module was designed specifically to detect carbon radiation as a demonstration of our approach. Nitrogen can be detected by substituting a second multilayer optic designed to discriminate and transport the characteristic radiation of nitrogen. The multilayer x-ray optic was fabricated by pressing thin multilayer-coated silicon substrates into a cylindrical figured mandrel. The multilayer coating consisted of alternating layers of tungsten and carbon deposited by magnetron sputtering at ARACOR. The theoretical bandpass response, shown in figure 3, provides a peak reflectivity for carbon radiation of almost 10 percent. In contrast, the oxygen signal should be reduced by four orders of magnitude.

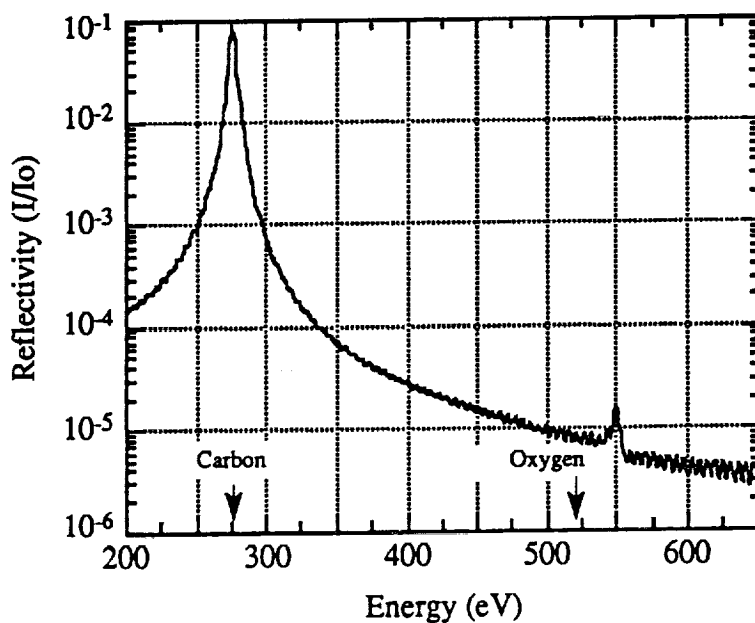


Figure 3.- Multilayer bandpass response for carbon.

The light-element fluorescence breadboard module is illustrated in figure 4. The multilayer optic collects the carbon fluorescent radiation and transports it to an x-ray detector. A thin window gas flow proportional counter was selected for the breadboard demonstration for its energy resolving properties and to verify that the multilayer optical component effectively suppresses the oxygen radiation.

The carbon fluorescent radiation was produced by alpha particle excitation of the sample. We selected a 1 mCi polonium-210 alpha particle source on the basis of its ready availability. This source has a relatively short half-life of 138 days compared to the 360 day trip to Mars. In practice, a higher activity source with a longer half-life (on the order of 3 years) would be used.

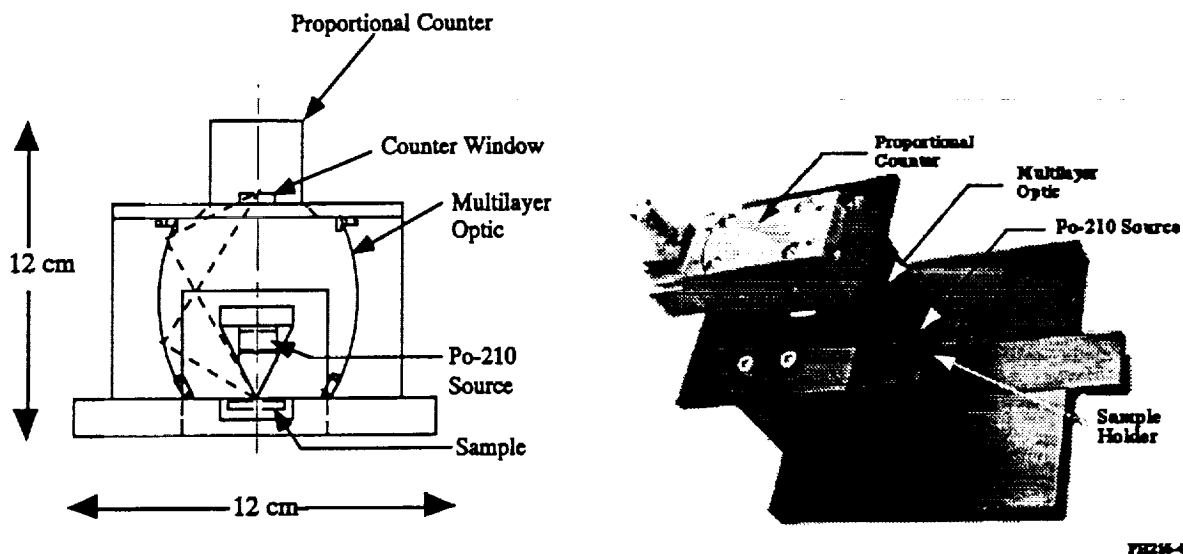


Figure 4.- The light element x-ray fluorescence breadboard module.

The distance from the source to the sample was about 1.5 cm, and the sample to detector distance was approximately 7 cm. The required sample size was on the order of 0.5 g.

### 2.3 Supporting Auxiliary Equipment

The breadboard operations were performed in a vacuum chamber that doubled as a radiation shield. This chamber could be back-filled with CO<sub>2</sub> to simulate the Martian atmosphere. We also regulated the temperature inside the chamber and could reduce it to simulate the nocturnal Martian ambient temperature of about -50 °C. The CCD was thermoelectrically cooled and waste heat was transported through the vacuum chamber by a closed cycle refrigeration system. The CCD was controlled with a personal computer that also performed data analysis to produce the measured diffraction line profiles and fluorescent spectra. We also instrumented the x-ray tube with thermocouples to monitor its temperature rise during operation in vacuum or in the rarefied CO<sub>2</sub> atmosphere.

The light element fluorescent breadboard unit was supported by a gas handling system that delivered a well controlled amount of propane to the gas flow proportional counter. The proportional counter required a source of high voltage as well as a spectroscopy data acquisition system. A multichannel analyzer was used to display the measured light element spectra.

### 3.0 BREADBOARD DEMONSTRATION

The breadboard demonstration experiments were designed to determine some of the performance parameters of the breadboard modules, such as spectral and d-spacing resolution. Further, they demonstrated that the module could span the d-spacing range from 1.8 to 20 Å, distinguish between amorphous and crystalline constituents, and detect fluorescence over the elemental range from carbon through uranium. The following subsections present these results for each analytical technique.

#### 3.1 X-ray Diffraction Breadboard Results

We examined a series of pure crystalline samples, such as halite, to determine the performance of the x-ray diffraction breadboard module in terms of the d-spacing resolution and signal-to-background ratio. We then examined montmorillonite and for palagonite/crystalline samples prepared by NASA Ames to demonstrate the performance of the breadboard diffraction module. These data were all obtained with 1 W of power dissipated at the x-ray tube anode (for an input power of 3.5 W). The breadboard demonstration experiments were performed in a simulated Martian environment, represented by an atmosphere of 8 Torr of dry CO<sub>2</sub> and an ambient temperature of -50°C.

##### *X-Ray Diffraction Breadboard Characterization*

The d-spacing and background performance of the diffraction breadboard module was characterized by the examination of a variety of pure minerals. These data were all obtained with an examination time of 320 seconds. Figure 5 shows representative data obtained by the examination of the most intense peak of halite located at a d-spacing of 2.82 Å. These data indicate that the signal-to-background ratio is about 100 to 1. Further, the d-spacing resolution is about 0.064 Å at a d-spacing of 2.82 Å, yielding a value of  $d/\Delta d$  of 44. This is favorably compared to the theoretical  $d/\Delta d$  of 42 presented in figure 2.

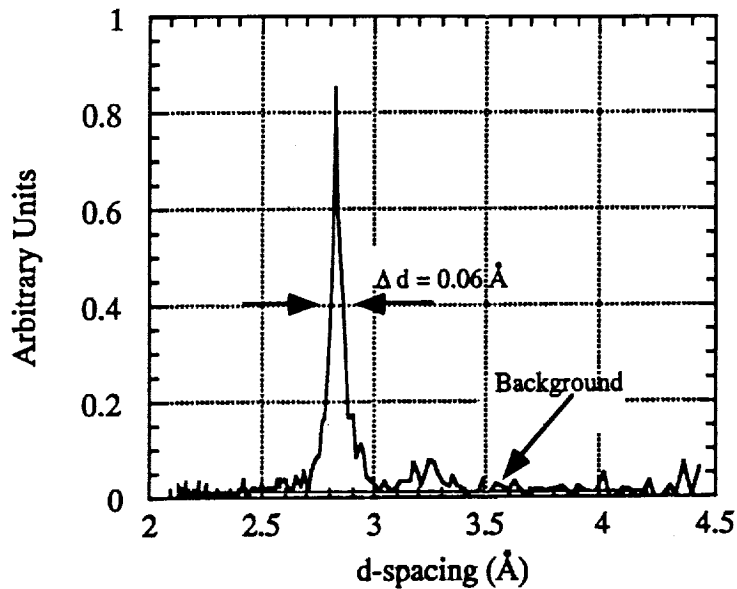


Figure 5.- Breadboard x-ray diffraction examination of halite.

We then characterized the performance of the breadboard module by the examination of complex minerals that are made up of multiple closely related constituents. Typical of the data obtained are the results for montmorillonite, a complex weathered clay, made up of five constituents. The diffraction pattern obtained by the examination of montmorillonite is shown in figure 6. This pattern was obtained with the CCD positioned to first record the diffraction pattern characteristic of d-spacings from 2 to 4 Å and then translated to record the diffraction pattern for d-spacings from 4 to 22 Å.

The observed d-spacings are compared to the tabulated d-spacings of all montmorillonite species, obtained from the International Center for Diffraction Data (ICDD) file (reference 4), in table 2. The major montmorillonite constituents, corresponding to d-spacings of 2.5, 2.6, 3.1, and 4.5 Å were identified.

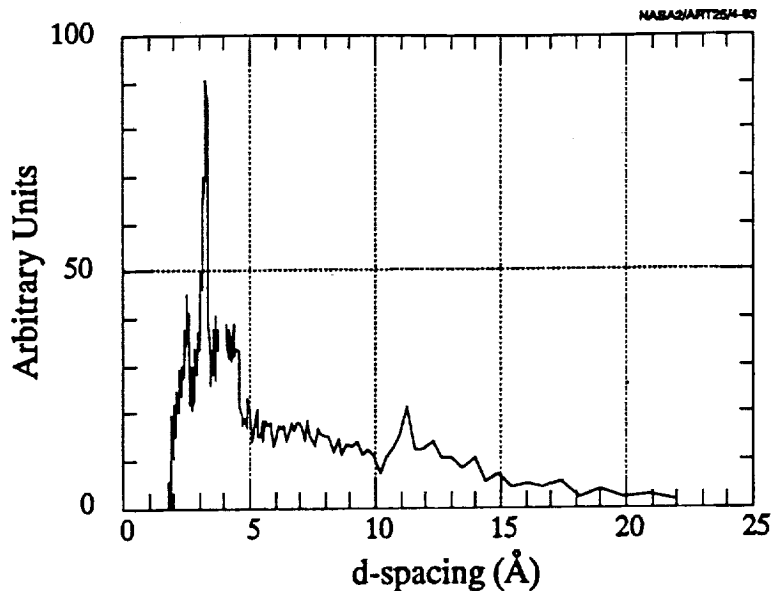


Figure 6.- Breadboard x-ray diffraction examination of montmorillonite.

TABLE 2. OBSERVED AND TABULATED MONTMORILLONITE D-SPACINGS.

Observed d-spacing (Å)	Tabulated d-spacing (Å)	ICDD File Number
(2.5,3.1,4.5,11.2)	(3.2, 3.3, 4.5, 13.6)	13-259
	(2.6, 3.1, 4.5, 13.6)	13-135
	(3.0, 4.5, 5.0, 15.0)	29-1498
	(1.5, 3.1, 4.5, 21.5)	12-219
	(2.5, 3.1, 4.5, 21.5)	29-1499

The data in figure 6 (and tabulated in table 2) illustrate that significant information about the composition of the montmorillonite sample can be obtained with the d-spacing resolution of the diffraction breadboard. The data also illustrate that the location of the peak is very sensitive to the sample tilt angle and the location of the CCD. This can be seen by noting the location of the peaks in the data covering the range from 4 to 22 Å. Note that the peak at 13.6 Å appears at a d-spacing that is about 11 Å, a shift commensurate with the accuracy of re-setting the sample tilt angle and the CCD location. The characteristic peak at 13.6 Å appear broadened as a result of the d-spacing resolution of about 2.3 Å achieved by the breadboard. The peaks at 15 and 21.5 Å are not observable due to the d-spacing resolution of the module.

### *Palagonite/Crystalline Test Samples*

NASA Ames prepared a series of samples to test the performance of the breadboard module. These samples were designed to demonstrate the sensitivity of the breadboard module as well the dependence of the diffraction signal with mineral concentration. The crystalline component of the test samples was made up of a complex mixture minerals listed in table 3.

TABLE 3. CRYSTALLINE TEST MATRIX.

Constituent	Weight Percent
Nontronite	20
Montmorillonite	20
Iron-Rich Montmorillonite	20
Thenardite	15
Aragonite	5
Siderite	5
Farringtonite	5
Calcite	5
Nitratine	2.5
Magnetite	1.25
Maghemite	1.25

This crystalline mixture was mixed with palagonite, a basaltic rock with a large concentration of glass, to produce a range of mineral and amorphous concentrations. Ames provided us with mineral samples composed of 50, 80, and 90 percent palagonite by weight.

These samples were examined for periods ranging from 30 to 60 minutes by the breadboard diffractometer. The resulting diffraction patterns for the 50, 80, and 90 percent palagonite are shown in figures 7, 8, and 9 respectively. Figure 7 also contains, for the purposes of comparison, a high resolution scan of the 50% palagonite sample obtained with a commercial diffractometer (and a power level of 500 W). The d-spacing resolution,  $d/\Delta d$ , achieved by this diffractometer is approximately 150 at a d-spacing of 2.8 Å. Going from the commercial diffractometer to the breadboard module, the resolution scales roughly with the diffractometer

radius as anticipated. Given the differences in d-spacing resolution, the breadboard reproduced all major features present in the high resolution diffractometry scan.

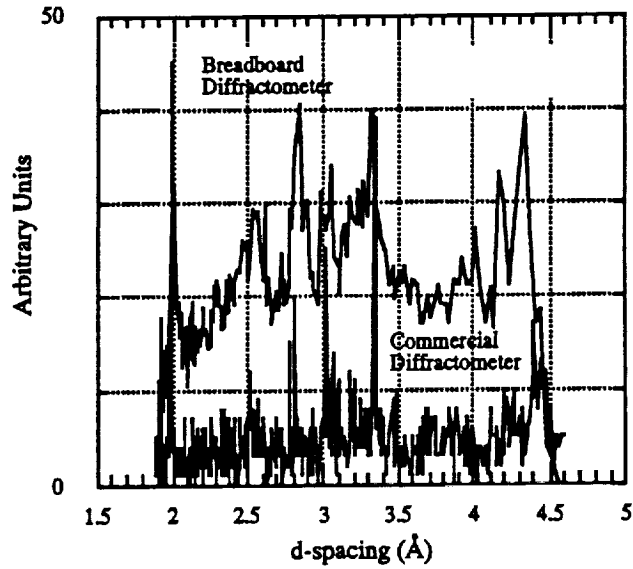


Figure 7.- Breadboard x-ray diffraction examination of 50% palagonite.

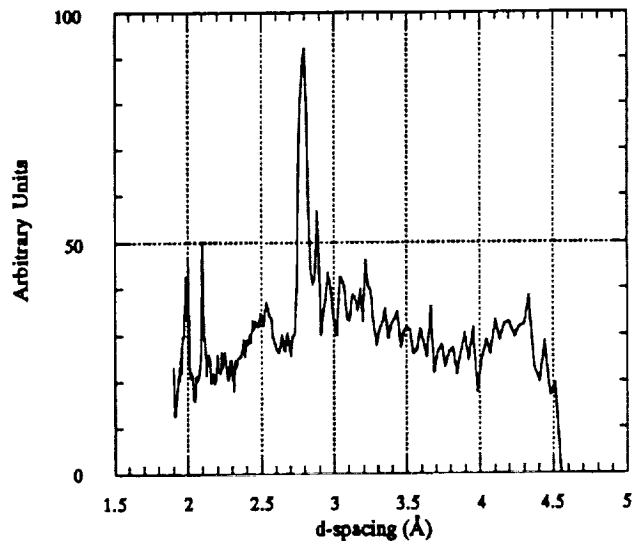


Figure 8.- Breadboard x-ray diffraction examination of 80% palagonite.

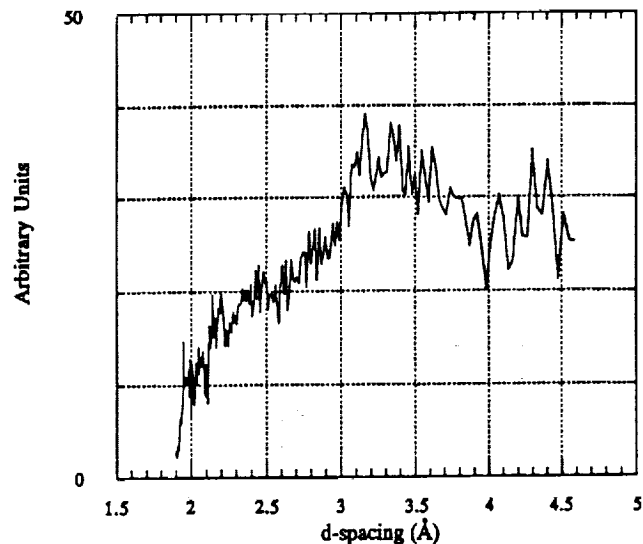


Figure 9.- Breadboard x-ray diffraction examination of 90% palagonite.

The diffraction data in figures 7 to 9 are displayed on a common scale. Note that there is no direct relationship between the amount of crystalline material and the magnitude of the diffraction peaks. This can be most clearly seen by comparing the intensities of the peak at 2.65 Å in the 50% palagonite sample and the 80% palagonite sample. This is a direct consequence of the random orientation of the sample grains and the lack of sample motion which would average out these effects.

We can, however, identify a number of peaks that are associated with the specific minerals present in the sample, even with the lack of sample motion. The d-spacings observed for the 50% palagonite sample are tabulated in table 4 along with the candidate mineral that they represent. The d-spacing resolution of the breadboard module is sufficient to identify peaks that are characteristic of all of the minerals listed in table 3.

The data indicate a diffraction line at 2.32 Å that is characteristic of nitratine. This mineral is present at the 2.5 weight percent level in crystalline test matrix that is mixed in equal proportions with palagonite to form the 50% palagonite sample. Thus, the data suggest that the minimum detectable level is approximately 1 weight percent.

TABLE 4. OBSERVED AND TABULATED D-SPACINGS IN 50% PALAGONITE SAMPLE.

Observed d-spacing (Å)	Mineral	Tabulated d-spacing (Å)
1.90, 1.93	Nitratine, Calcite	1.9, 1.91
1.96, 1.99	Halite, Aragonite	1.98, 1.99
2.09	Calcite	2.1
2.29	Calcite	2.29
2.32	Nitratine	2.31
2.42	Farringtonite	2.41
2.53	Magnetite, Maghemite	2.52, 2.53
2.57, 2.62	Nontronite (34-842, 29-1497) Montmorillonite (13-135, 29-1499)	2.56, 2.6 2.56, 2.56
2.72	Aragonite	2.7
2.78	Thenardite, Siderite	2.78, 2.8
2.84	Halite, Nitratine	2.82, 2.81
2.93	Maghemite	2.95
2.98	Magnetite	2.97
3.05	Montmorillonite (29-1498), Nitratine, Calcite, Thenardite	3.02 3.03, 3.04, 3.08,
3.14	Montmorillonite (13-135)	3.13
3.17	Montmorillonite (29-1499), Thenardite	3.15
3.23	Montmorillonite (13-259)	3.23
3.27	Halite, Aragonite	3.26, 3.27
3.32	Montmorillonite (13-259)	3.34
3.46	Aragonite, Farringtonite	3.4, 3.44
3.55, 3.6	Nontronite(29-1497), Siderite	3.58, 3.59
3.82	Farringtonite	3.85
4.32	Farringtonite	4.36
4.44	Montmorillonite (29-1499, 13-135, 13-259, 12-219)	4.45, 4.46, 4.47, 4.49

Comparison of diffraction data obtained by the breadboard for these samples also demonstrates a characteristic signature associated with amorphous materials. High resolution diffractometry of a 100 percent palagonite sample (with a conventional laboratory diffractometer operating at an x-ray tube power of 1.4 kW) indicated that the amorphous signature appears as a broad peak centered at a d-spacing of 3.2 Å. The amorphous signal does not depend on the grain size or orientation and thus it should scale directly with concentration.

The peak amorphous signal levels at 3.2 Å, expressed in arbitrary units, are 23 and 34 for the 50% and 80% palagonite samples, respectively. Thus, the signal level increased by a factor of about 1.5 for an increase in the palagonite fraction of 1.6. A more quantitative determination of the relationship between the amorphous signal level and the concentration will require the isolating the amorphous signal from the characteristic diffraction lines.

## 3.2 X-Ray Fluorescence Breadboard Results

The performance of the standard range x-ray fluorescence module was characterized by measurement of the energy resolution of the CCD and by the spectroscopic examination of a montmorillonite sample. The light element x-ray fluorescence module was characterized by evaluation of the ability of the multilayer bandpass optics to discriminate against oxygen radiation, and observation of carbon fluorescence radiation signals as a function of carbon concentration in a mineral matrix.

### *Standard Range X-Ray Fluorescence Breadboard Characterization*

The energy resolution of the CCD was determined by examining the characteristic x-ray emissions with energies from 1.4 keV through 22 keV. The full width at half maximum of the photopeak at an x-ray energy of 5.9 keV (produced by an iron-55 isotopic source) was 340 eV. This resolution is between the nominal resolution of high quality proportional counters (about 500 eV) and cooled Si(Li) detectors (about 100 eV). Our resolution performance was limited primarily by the data acquisition system that is commercially supplied with the CCD camera. Other workers have demonstrated energy resolutions comparable to that of a Si(Li) detector when the CCD data acquisition system is optimized for spectroscopy rather than imaging applications.<sup>6</sup>

The x-ray fluorescence spectra of the montmorillonite sample is shown in figure 10. The iron x-ray tube excited the fluorescence from elements lighter than iron. The Cd-109 isotopic x-ray source excited the fluorescence of the elements primarily above iron. These data indicate that the CCD is sensitive to x-rays with energies from about 1 keV through 27 keV. This range is sufficient to detect the K and L emissions of all elements from sodium to uranium. The lower energy cutoff at sodium is due to the noise level (approximately 37 electrons) of the CCD, a consequence of the data acquisition system.

These data also demonstrate the ability of a combined instrument to provide explicit mineral identification. The fluorescence spectrum from montmorillonite sample contains a large calcium peak. This peak can be used to identify the presence of the only montmorillonite type containing calcium (ICDD file no. 29-1498). The diffraction data, shown in figure 6, indicated that all of the montmorillonite types were present in the sample.

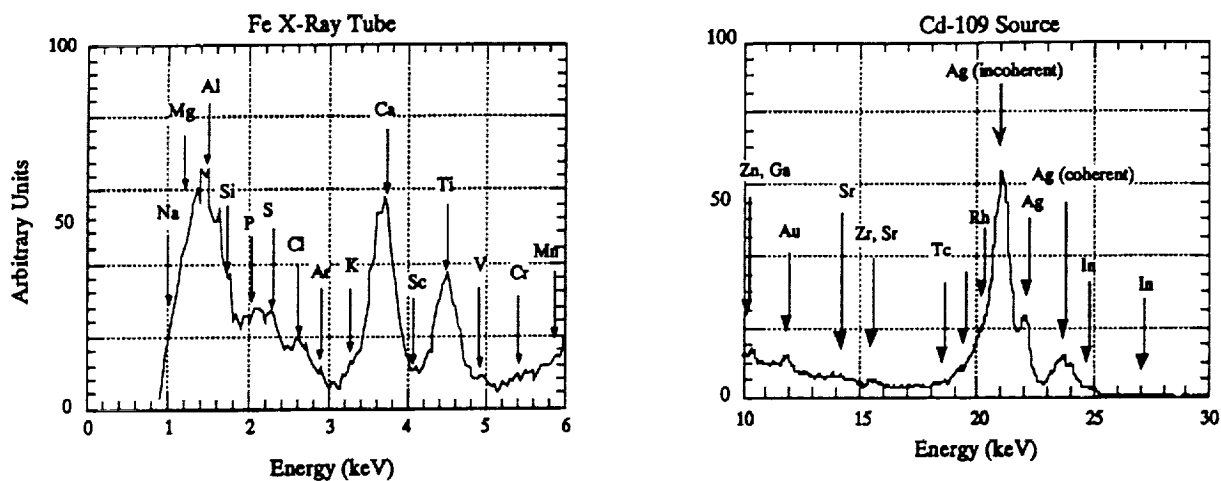
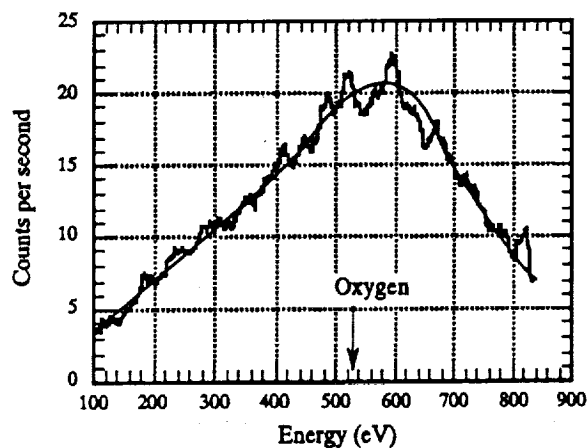


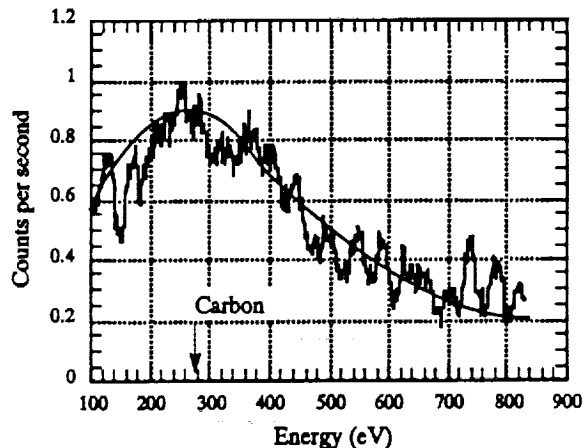
Figure 10.- Breadboard x-ray fluorescence examination of montmorillonite.

*Light Element X-Ray Fluorescence Breadboard Characterization*

We demonstrated that the multilayer optic provides bandpass discrimination by recording the fluorescence produced through alpha particle excitation from a calcium carbonate ( $\text{CaCO}_3$ ) sample with the gas flow proportional counter looking at the sample directly and through the optic. The resulting spectra are compared in figure 11. The  $\text{CaCO}_3$  fluorescence spectrum is dominated by the signal from oxygen. The width of the spectrum indicates that there are other emissions that are contributing to the signal even though they are not resolved. The carbon emission is not readily visible when the detector views the sample directly, given the magnitude of the oxygen signal.



(a)  $\text{CaCO}_3$  fluorescence spectrum



(b) Multilayer optic filtered spectrum

Figure 11.- Demonstration of bandpass rejection of oxygen.

The spectrum transported by the multilayer optic, on the other hand, shows that the oxygen is effectively suppressed. The width of the measured carbon spectra is a consequence of the spectral resolution of the proportional counter. The demonstration of oxygen suppression is an important result since it demonstrates that a non-energy resolving detector can be used in the integrated instrument.

We calibrated the light element x-ray fluorescence module by examination of thin carbon films whose thicknesses ranged from 10 to 2,000 Å and from a pure, thick carbon sample. We removed the multilayer optic and deployed the proportional counter to view the calibration films directly to increase the collection solid angle. The proportional counter window and the gas pressure were adjusted to reduce the detection efficiency of oxygen radiation. This had only a minor impact on the quantum efficiency for carbon radiation.

NASA Ames provided us with test samples made up of palagonite spiked with trace amounts (0.01, 0.1, and 1 weight percent) of bovine serum albumin (BSA). NASA Ames analyzed the chemical makeup of BSA to determine that it is 97 percent carbon. Figure 12 presents the thin carbon film data along with the data obtained from the palagonite test samples spiked with 0.1 and 1 weight percent BSA. It also shows, by the curve, the theoretical dependence of the carbon fluorescence signal as a function of thickness. Excellent agreement is noted between the test samples and the calibration samples and the theoretical dependence of the signal levels.

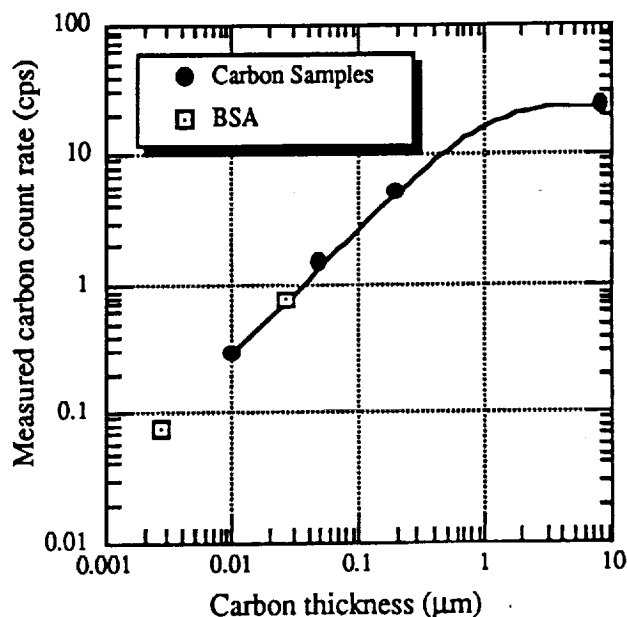


Figure 12.- Carbon signal as a function of concentration.

Note that the 0.1 wt percent BSA sample corresponds to a carbon concentration of 1000 ppm. Achieving a lower detection limit of 100 ppm in an observation period of 4.5 hours for carbon requires that the radioisotope source strength be increased by a factor of about 30. Radioactive sources of this activity are available on a custom manufacturing basis.

### 3.3 Compatibility with Planetary Exploration Constraints

This section considers the plausibility that the integrated x-ray instrument can be made compatible with the constraints associated with planetary exploration. The evaluation of compatibility is made by reference to the mass, volume, power constraints listed in Table 1.

The breadboard demonstration experiments were all performed in less than 4.5 hours implying compliance with this performance design specification.

The breadboard modules currently do not meet the mass specification of less than or equal to 2.5 kg. The mass of the two modules is 4.5 kg, not including the mass of auxiliary support systems. Thus, it is plausible that the mass can be reduced through additional integration to meet the constraint of 2.5 kg listed in table 1.

Similarly, the two breadboard modules, if placed side by side, have total external dimensions (L x W x H) of 25 x 15 x 10 cm<sup>3</sup>. This satisfies the volume constraint of 0.1 m<sup>3</sup>. The bulkiest of the required support subsystems are the CCD cooling system and the data acquisition computer. Active CCD cooling is not required on Mars since this unit is intended to be operated during the Martian night at an ambient temperature of about -50 °C. The data acquisition function can be provided by specialized compact CCD hardware developed by NASA for planetary exploration.<sup>7</sup> Thus, satisfaction of the volume constraint appears plausible.

The breadboard modules currently do not meet the 15 W power constraint of table 1. The breadboard modules require approximately 35 W (4 W for the x-ray tube, 30 W for the CCD, and 1 W for the light element detector). The CCD power requirements are a direct consequence of the fact that this unit was developed for commercial applications and not for planetary exploration. We believe that the CCD power requirement can be reduced to a level of about 3 W.<sup>7</sup> Thus, it is plausible to believe that the x-ray tube, CCD detector, and the light element detector can be operated on approximately 8 W. This leaves 7 W for sample motion and other supporting functions.

On the basis of the mass, volume, and power levels of the breadboard modules, we believe that it is plausible that the integrated x-ray laboratory can be made compatible with the constraints listed in table 1.

#### 4.0 CONCLUSIONS/RECOMMENDATIONS

We have demonstrated the feasibility that x-ray fluorescence and x-ray diffraction capabilities can be incorporated into an instrumentation package that meets the nominal mass, volume, power constraints associated with *in situ* planetary exploration. This demonstration was obtained by the fabrication of x-ray fluorescence and diffraction breadboard modules and subsequent testing and calibration to validate the analytical basis for the concept.

The breadboard diffraction module was designed to cover a d-spacing range from 1.5 to 20 Å. A larger CCD (with 1024 x 1024) pixel elements could allow the entire range of d-spacings to be sampled in a single measurement. We verified that our performance prediction models accurately predicted the d-spacing resolution. Further, the levels of background are sufficiently low that they do not significantly affect the quality of the diffraction data. We have demonstrated that we can identify the presence of minerals in a complex mixture that is representative of purported Martian soil conditions. The breadboard experiments demonstrated that the mineral detection limit is about 1 weight percent in a complex mixture of elements. Further, we demonstrated that the amorphous signal level scales approximately linearly with the amorphous material concentration.

Extracting quantitative information about the concentration of the minerals requires additional effort. First, improving the d-spacing resolution will allow closely spaced peaks to be individually resolved, thus improving the accuracy with which the minerals can be identified. This can be achieved by reducing the size of the individual pixels of the CCD and by increasing the diffractometer radius. Second, incorporating sample motion into the x-ray diffraction breadboard will average the effect of preferential grain orientation. This should make the diffraction signal scale linearly with concentration.

The standard-range x-ray fluorescence breadboard module demonstrated the potential to detect elements from sodium through uranium. The detection limits achieved by the breadboard remain to be quantified and thus we did not demonstrate the ability to detect elements to lower detection limits of 100 ppm. The selection of a commercially available CCD for use in the breadboard limited its performance as a fluorescence analyzer. The data acquisition system was designed primarily for imaging and not for spectroscopy applications, and thus the CCD was characterized by a noise level of 37 electrons. This affected the energy resolution of the breadboard and restricted the lowest detectable element to sodium (creating a gap in coverage from the elements oxygen to sodium).

The noise level and the energy resolution of the CCD can be dramatically improved by incorporating a data acquisition system designed specifically for spectroscopy. There are existing designs that have characteristic noise levels on the order of 1 electron. These noise levels are sufficient to achieve CCD spectral resolution that is comparable to a high quality cooled Si(Li) detector. Additionally, the lower energy limit of the CCD would be reduced, to allow the observation of the characteristic emissions elements as light as carbon. The application of spectrum stripping and peak search routines will enhance the ability of the module to determine the concentration of elements in the sample.

The light element x-ray fluorescence breadboard demonstrated that the energy resolution provided by the multilayer optics effectively suppresses the signal from the interfering fluorescence of oxygen. Thus, a non-energy resolving detector can be used for this application. This will ultimately simplify the design of the module by reducing the complexity of the data acquisition system. The measured signal levels indicated that approximately a factor of 30 increase in source strength is required to assay carbon at the 100 ppm level. This increase is feasible, and thus this detection limit is readily achievable.

Given the experience with the breadboard modules, we believe that it is plausible for an integrated x-ray diffraction and fluorescence laboratory to meet constraints associated with planetary exploration missions. Further development of the instrument should be tied to a specific mission from which we can address a set of science objectives. This will determine, for example, if further effort should be spent on improving the d-spacing resolution of the x-ray diffraction breadboard. This effort relied on the MESUR mission to Mars as a baseline mission to set the overall instrument constraints for the development of the breadboard. Support for continued near term instrument development is recommended to provide this capability for projected ARTEMIS lunar and MESUR Mars missions projected for the late 1990's.

## 5.0 REFERENCES

1. Goals for the Exploration of Mars. Mars Science Working Group. NASA, Washington, DC., 1986.
2. Strategy for the Exploration of the Inner Planets. Committee of Planetary and Lunar Exploration. National Academy of Sciences, Washington, DC, 1978.
3. Planetary Exploration Through the Year 2000: An Augmented Program. Solar System Exploration Committee. NASA, Washington, DC, 1986.
4. Powder Diffraction File. International Centre for Diffraction Data, Swathmore, PA, 1991.
5. Hubbard, G. S., Wercinski, P. F., Sarver, G. L., Hamel, R. P., and Ramos, R. A Mars Environmental Survey (MESUR) - Feasibility of a Low Cost Global Approach. Presented at the 42nd Congress of the International Astronautical Association, 1991.
6. Janesick, J.
7. Janesik, J personal communication

# REPORT DOCUMENTATION PAGE

Form Approved  
OMB No. 0704-0188

Public reporting burden for this collection of information is estimated to average 1 hour per response, including the time for reviewing instructions, searching existing data sources, gathering and maintaining the data needed, and completing and reviewing the collection of information. Send comments regarding this burden estimate or any other aspect of this collection of information, including suggestions for reducing this burden, to Washington Headquarters Services, Directorate for Information Operations and Reports, 1215 Jefferson Davis Highway, Suite 1204, Arlington, VA 22202-4302, and to the Office of Management and Budget, Paperwork Reduction Project (0704-0188), Washington, DC 20503.

1. AGENCY USE ONLY (Leave blank)	2. REPORT DATE December 1993	3. REPORT TYPE AND DATES COVERED Contractor Report	
4. TITLE AND SUBTITLE Demonstration of the Feasibility of an Integrated X-Ray Laboratory for Planetary Exploration		5. FUNDING NUMBERS  NAS2-13416	
6. AUTHOR(S) E. D. Franco, J. A. Kerner, L. N. Koppel, and M. J. Boyle		8. PERFORMING ORGANIZATION REPORT NUMBER  A-94033	
7. PERFORMING ORGANIZATION NAME(S) AND ADDRESS(ES) Advanced Research and Applications Corporation 425 Lakeside Drive Sunnyvale, CA 94086		10. SPONSORING/MONITORING AGENCY REPORT NUMBER  NASA CR-177631	
9. SPONSORING/MONITORING AGENCY NAME(S) AND ADDRESS(ES) National Aeronautics and Space Administration Washington, DC 20546-0001		11. SUPPLEMENTARY NOTES Point of Contact: M. L. Fonda, Ames Research Center, MS 239-12, Moffett Field, CA 94035-1000 (415) 604-5744	
12a. DISTRIBUTION/AVAILABILITY STATEMENT  Unclassified — Unlimited Subject Category 88		12b. DISTRIBUTION CODE	
13. ABSTRACT (Maximum 200 words)  The identification of minerals and elemental composition is an important component in the geological and exobiological exploration of the solar system. X-ray diffraction and fluorescence are common techniques for obtaining these data. This project demonstrated the feasibility of combining these analytical techniques in an integrated x-ray laboratory compatible with the volume, mass, and power constraints imposed by many planetary missions. In this project, breadboard level hardware was developed to cover the range of diffraction lines produced by minerals, clays, and amorphous; and detect the x-ray fluorescence emissions of elements from carbon through uranium. These breadboard modules were fabricated and used to demonstrate the ability to detect elements and minerals. Additional effort is required to establish the detection limits of the breadboard modules and to integrate diffraction and fluorescent techniques into a single unit. We conclude that this integrated x-ray laboratory capability will be a valuable tool in the geological and exobiological exploration of the solar system.			
14. SUBJECT TERMS Fluorescence, X-ray diffraction, Planetary exploration		15. NUMBER OF PAGES 30	
		16. PRICE CODE A03	
17. SECURITY CLASSIFICATION OF REPORT Unclassified	18. SECURITY CLASSIFICATION OF THIS PAGE Unclassified	19. SECURITY CLASSIFICATION OF ABSTRACT	20. LIMITATION OF ABSTRACT

